

T D Swinburne, K Arakawa, H Mori, H Yasuda, M Isshiki, K Mimura,
M Uchikoshi, and S L Dudarev

Fast, vacancy-free climb of prismatic dislocation loops in bcc metals

Enquiries about copyright and reproduction should in the first instance be addressed to the Culham Publications Officer, Culham Centre for Fusion Energy (CCFE), K1/083, Culham Science Centre, Abingdon, Oxfordshire, OX14 3DB, UK. The United Kingdom Atomic Energy Authority is the copyright holder.

Fast, vacancy-free climb of prismatic dislocation loops in bcc metals

T D Swinburne,¹ K Arakawa,² H Mori,³ H Yasuda,³ M Isshiki,⁴ K Mimura,⁴
M Uchikoshi,⁴ and S L Dudarev¹

¹*CCFE, Culham Science Centre, Abingdon, Oxon, OX14 3DB, UK*

²*Department of Materials Science, Faculty of Science and Engineering, Shimane University, 1060
Nishikawatsu, Matsue 690-8504, Japan*

³*Research Center for Ultra-High Voltage Electron Microscopy, Osaka University, 7-1 Mihogaoka,
Ibaraki, Osaka 567-0047, Japan*

⁴*Institute of Multidisciplinary Research for Advanced Materials, Tohoku University, 2-2-1
Katahira, Aoba-ku, Sendai 980-8577, Japan*

Fast, vacancy-free climb of dislocation loops in bcc metals

T D Swinburne,¹ K Arakawa,² H Mori,³ H Yasuda,³ M Isshiki,⁴ K Mimura,⁴ M Uchikoshi,⁴ and S L Dudarev¹

¹*CCFE, Culham Science Centre, Abingdon, Oxon, OX14 3DB, UK*

²*Department of Materials Science, Faculty of Science and Engineering,
Shimane University, 1060 Nishikawatsu, Matsue 690-8504, Japan*

³*Research Center for Ultra-High Voltage Electron Microscopy,
Osaka University, 7-1 Mihogaoka, Ibaraki, Osaka 567-0047, Japan*

⁴*Institute of Multidisciplinary Research for Advanced Materials,
Tohoku University, 2-2-1 Katahira, Aoba-ku, Sendai 980-8577, Japan*

(Dated: March 22, 2016)

Vacancy mediated climb mechanisms cannot account for the fast, direct coalescence of prismatic dislocation loops observed in nuclear materials at low to intermediate homologous temperatures. We quantitatively develop an alternative ‘self climb’ model, where climb occurs due to pipe diffusion around the loop perimeter, independent of the vacancy atmosphere and thus the vacancy formation energy. Molecular statics calculations show the energy landscape for pipe diffusion can be captured by a simple bond counting model, which, using kinetic Monte Carlo simulations, yields an effective activation energy for self climb of 2 to 2.5 times the vacancy migration energy depending on dislocation character. Dislocation dynamics allowing self climb and glide show quantitative agreement with transmission electron microscopy observations, demonstrating that this novel form of vacancy-free climb is many orders of magnitude faster than traditional climb models. Implications for the coarsening rates of defect networks are explored.

Dislocation glide dominates plastic flow at low homologous temperatures, but confinement to a glide surface significantly restricts the evolution of a defect network[1]. Dislocation climb, which requires concurrent mass transport, is typically much slower than glide but allows migration off the glide surface, giving rise to a wide range of important plasticity mechanisms including network coarsening[2, 3] and creep[4]. Climb is known[5–9] to be particularly important in post-irradiation annealing, accelerating the coalescence (after an initial recombination phase) of the many small self interstitial atom (SIA) and vacancy clusters produced in a cascade event into larger dislocation loops and dislocation lines, increasing the cell size of a dislocation network and transforming the mechanical response of materials. For this reason accurate inclusion of climb motion is highly desirable to avoid the artificially restricted dynamics of glide-only dislocation models, particularly for applications at elevated temperatures.

The most widely studied atomic mechanism for climb transports mass through a pre-existing vacancy atmosphere, either at an equilibrium concentration or in supersaturation due to irradiation[3], with dislocations acting as perfect sources and sinks for vacancies[2, 4]. By emitting and absorbing vacancies, dislocation segments can move off their glide plane; in addition, as the self stress of a dislocation loop is approximately proportional to the inverse of the loop radius[1], larger loops tend to grow at the expense of smaller loops (whilst maintaining the equilibrium vacancy concentration) a feature that is clearly observable in experiment[7]. As the vacancy current at a dislocation is proportional to the product of the vacancy concentration and diffusivity $c_V D_V$, the rate of VMC is controlled by the large activation energy

$E_f^V + E_m^V$ for vacancy formation and migration[3], meaning VMC mechanisms are only expected to be active at large homologous temperatures[4].

However, it has long been recognized[5–7, 9, 10] that prismatic loops can migrate away from their glide surface, with no observable change in size, until directly coalescing with neighboring loops. The climb motion in this case is clearly not VMC as the loop area is conserved; furthermore, we confirm previous findings[5, 9, 11] that the observed climb velocities are orders of magnitude larger than those predicted by VMC and active at much lower homologous temperatures, with important implications for microstructural evolution. An alternative ‘self climb’ model has been proposed to account for these puzzling observations[5, 10]. In self climb, loops are able to migrate in their habit plane due to the diffusion of self interstitial atoms in the loop around the loop perimeter, in close analogy to the diffusion mechanism of large adatom islands[12]. As no vacancy atmosphere is required in self climb, the mobility is suspected to be much greater than VMC as a factor $c_V = \exp(-\beta E_f^V)$ is absent. Despite the first proposal of this mechanism over five decades ago and the clearly observable rôle of self climb in dislocation coarsening, there has not been any quantitative development of a self climb mobility, resulting in its absence from microstructural models.

In this paper, we employ molecular statics to investigate possible structural fluctuations of SIA loops that are then encoded for kinetic Monte Carlo (KMC) simulations to construct a simple mobility law for dislocation self climb, parametrized only by the vacancy migration energy E_m^V and the attempt frequency ν for vacancy migration. Our main result is that the activation energy for self climb is $(2 - 2.5)E_m^V$ depending on loop character, compared to

the VMC activation energy of $E_f^V + E_m^V \sim (3 - 5)E_m^V$ in bcc metals[13]. In fcc metals $E_f^V + E_m^V \sim (2 - 3)E_m^V$ [14], implying that self climb and VMC may be of comparable magnitudes, a question we leave for a future investigation. The consequent implication that self climb is active at much lower homologous temperatures than vacancy mediated climb (VMC) in bcc metals is confirmed through *in situ* transmission electron microscopy (TEM) observations of SIA loops in iron, with isolated SIA loops seen to execute unbiased self climb diffusion perpendicular to their Burgers vector, whilst adjacent SIA loops directly coalesce through self climb, driven by elastic interaction forces. We also analyze previously published observations of SIA loop coalescence in tungsten[9]. The measured diffusivities and coalescence times are around six orders of magnitude faster than those predicted by VMC models and in good agreement with dislocation dynamics simulations which allow self climb and glide, using the simple self climb mobility law

$$M_{\text{scl}} = \frac{2\beta\nu a^5}{\pi R^3} e^{-\beta\epsilon E_m^V}, \quad (1)$$

where $\beta = 1/k_B T$, $\epsilon = 2$ for $1/2\langle 111 \rangle$ loops, $\epsilon = 2.5$ for $\langle 100 \rangle$ loops, ν is the attempt frequency for vacancy diffusion, here taken from DFT calculations[15, 16], $R \simeq a\sqrt{N}/\pi$ the loop radius and a the lattice parameter. Whilst the form of (1) is similar to the result of Maher and Eyre[5], the current work provides the first quantitative calculation of the effective activation energy for self climb, the critical, rate controlling parameter, giving a robust self climb mobility law for use in dislocation plasticity models. We demonstrate the implications of self climb in bcc metals through with simple simulations of loop coarsening, which we compare to VMC.

Energy landscape for pipe diffusion in SIA loops As self climb is driven by pipe diffusion around the perimeter of SIA loops, we have simulated a large number (~ 100) of possible diffusion pathways for $1/2\langle 111 \rangle$ and $\langle 100 \rangle$ SIA loops in iron and tungsten, using the LAMMPS molecular simulation package[17] with empirical potentials by Gordon *et al.*[18] and Marinica *et al.*[19]. Dislocation loops were created by inserting a random palette of SIAs on (111) or (100) planes into a perfect lattice before a structural relaxation. Away from a so called ‘magic’ number of SIAs, loops cannot form perfect hexagons or squares, resulting in a geometrically necessary roughening of the loop perimeter which offers many possible migration pathways; we note that these asperities will be present in any real dislocation loop, a point of interest for studies of impurity pinning and other interaction processes. Possible migration pathways were investigated by selecting at random SIAs on the perimeter of a palette, then translating the selected SIA by an $a/2\langle 111 \rangle$, $a\langle 100 \rangle$ or $a\langle 1\bar{1}0 \rangle$ lattice vector to another perimeter position before a further relaxation. As the SIA atoms are already in off-lattice positions, a lattice vector translation also

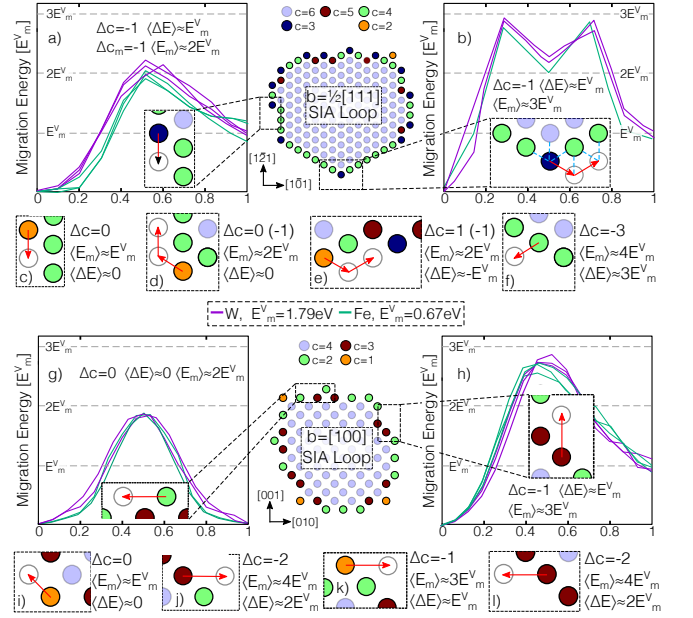


FIG. 1. A representative sample of energy barriers for self climb of $1/2\langle 111 \rangle$ and $\langle 100 \rangle$ prismatic loops in iron and tungsten. Defining a ‘bond’ as a nearest SIA neighbor, we find a clear correlation between the bond number and the expected migration barrier and total energy change, which can account for all observed pathways when normalized by the vacancy migration barrier (see main text for details).

finds an off lattice position. The nudged elastic band method[20] was then used to calculate the energy barrier between the two configurations, taking caution to choose an indexing protocol that minimizes the converged energy barrier, overcoming any ambiguity over identification of ‘the’ SIA atom in the relaxed structure of a dislocation core. It was found that all relaxed pathways between metastable states could be approximated as $a/2\langle 111 \rangle$ translations for $1/2\langle 111 \rangle$ loops, and $a/2\langle 111 \rangle$ or $a\langle 100 \rangle$ translations for $\langle 100 \rangle$ loops. As shown in Figure 1, after normalizing by the vacancy migration energy E_m^V for the interatomic potential, we find that the total change in energy ΔE and migration barrier E_m for a jumping atom can be accurately modeled simply by counting the number c of nearest SIA neighbors along the path, i.e. for each point on the path, $c = \sum_{j \neq i} \Theta(\sqrt{3}a/2 - |\mathbf{x}_i - \mathbf{x}_j|)$, where $\Theta(x)$ is the Heaviside step function. For SIAs in the interior of an $1/2\langle 111 \rangle$ loops $c = 6$, whilst for $\langle 100 \rangle$ loops $c = 4$; classifying the SIAs on a loop perimeter in this manner allowed us to produce the distribution of migration pathways shown in Figures 1a,b,f,g. Collating the results of our NEB calculations revealed the approximate relationship

$$\Delta E \simeq \Delta c E_m^V, \quad E_m \simeq (\Delta c + \sigma) E_m^V, \quad (2)$$

where $\sigma = 1$ for jumps along $a/2\langle 111 \rangle$ (c.f. Figures 1c and 1i) and $\sigma = 2$ for jumps along $a/2\langle 100 \rangle$ (c.f. Figure

1g). The remarkably simple relationship (2) can be rationalized by noting that vacancy migration along $a/2\langle 111 \rangle$ is, in a first approximation, the ‘breaking’ of a single nearest neighbors bond. An SIA in a SIA palette has an additional c such bonds, of which it must ‘break’ one in order to jump along $a/2\langle 111 \rangle$ and two to jump along $a\langle 100 \rangle$. In general, variations in the observed total energy change ΔE and migration barrier E_m were not observed to be greater than 15% from those predicted by (2), which typically overestimates E_m , thereby providing an upper bound on the self climb mobility. We also determined the effect of a nearby loop’s elastic field on the observed energy barriers by performing the same NEB calculations in the presence of another prismatic loop, rotating/inverting the loop of interest by a bcc symmetry operation to vary the elastic environment of the jumping atom. For loop separations of more than $\sim 5a$ we found variations in the energy barrier of less than 5%. As the goal of the above NEB calculations is to parametrize KMC simulations, an alternative approach to (2) would be to correlate all observed migration pathways for a given material with some detailed structural signature for the jumping atom involving second and third nearest neighbors, which could then be used to construct a large table of transition rates for use in KMC[21]. However, we believe our simple bond counting model (2) provides a high degree of quantitative accuracy (given the expected tolerances of the interatomic potential) coupled with an attractive simplicity that gives a universal model for self climb in bcc metals and allows the treatment of large, experimentally observable SIA loops.

Self climb mobility The inclusion of long range elastic interactions in KMC simulations is computationally demanding, as one is required to a great deal of transition rates on-the-fly, which are dependent on the entire system configuration. However, as the presence of a realistic external stress field was found to have only a weak influence over the measured migration barriers, we can calculate the self climb velocity \mathbf{v}_{cl} under a climb force \mathbf{F}_{cl} in the linear response regime $\mathbf{v}_{\text{cl}} = M_{\text{scl}}\mathbf{F}_{\text{cl}}$, where the self climb mobility is given by the Einstein relation $M_{\text{scl}} = \beta D_{\text{scl}}$. We therefore only need to calculate the self climb diffusivity D_{scl} of an isolated loops under no applied stress, a calculation that KMC is ideally suited to. We used the lattice KMC code KMCLIB[?] to simulate two dimensional self climb diffusion with state-state energy differences and migration barriers determined by (2), using energy units such that $E_m^V = 1$, with a hexagonal or square lattice for $1/2\langle 111 \rangle$ or $\langle 100 \rangle$ loops. The simulations produce a set $\{t_n, \bar{x}_n\}$ of center of mass positions $\bar{x} = \sum_i x_i/N$. By taking the mean squared displacement at sequentially greater time delays a diffusivity was extracted using established methods[22]. Our KMC simulations reveal (Figure 2) an effective activation energy $E_m = (2.0 \pm 0.07)E_m^V$ for $1/2\langle 111 \rangle$ SIA loops and $E_m = (2.5 \pm 0.03)E_m^V$ for $\langle 100 \rangle$ SIA loops, compa-

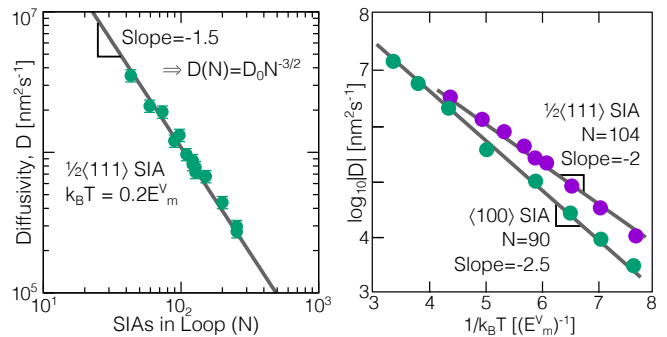


FIG. 2. Results from KMC simulations of SIA loop self climb. Left: log-log plot showing the $D_{\text{scl}} \propto N^{-3/2}$ relationship predicted by (3). Right: Arrhenius plots for $1/2\langle 111 \rangle$ and $\langle 100 \rangle$ SIA loops, giving clear activation energies of $2.0E_m^V$ and $2.5E_m^V$.

table to the energy barrier required for a lone SIA to traverse a corner or step on the loop perimeter (c.f. Figures 1d and 1k). The larger activation energy for $\langle 100 \rangle$ self climb can be attributed to the larger energy barrier for SIA migration along $\langle 100 \rangle$ directions, though in both cases the self-climb activation energy is much lower than that required for the ‘nucleation’ of lone SIAs from flat low index directions ($4E_m^V$ for both SIA loops, c.f. Figures 1f and 1l). KMC simulations, where such nucleation processes are explicitly forbidden, exhibit unchanged diffusivities, confirming that migrating SIAs are produced around corners or roughened structures on the loop perimeter. To derive an analytical expression for D_{scl} , we consider an isolated loop of N SIAs with an approximately circular shape, such that $N \simeq \pi R^2/a^2$. The center of mass diffusivity is given by $D_{\text{scl}} = \sum_{ij} D_{ij}/N^2$, where $D_{ij} = \lim_{t \rightarrow \infty} \langle \Delta x_i \Delta x_j \rangle / 2t$. As only $N_p \simeq 2\pi R/a$ SIAs on the perimeter are able to move ($D_{ij} \neq 0$), under the assumption of uncorrelated perimeter atoms we obtain

$$D_{\text{scl}} = \frac{N_p}{N^2} D_p = \frac{2a^5}{\pi R^3} \nu \exp(\beta E_m), \quad (3)$$

which with the Einstein relation $M_{\text{scl}} = \beta D_{\text{scl}}$ gives our main result, equation (1) for a self climb mobility. The predicted relationship $D_{\text{scl}} \propto R^{-3} \sim N^{-3/2}$ is in agreement with our simulations (Figure 2) and analysis of perimeter diffusion controlled transport of adatom islands[12].

TEM observations of SIA loops To validate our self-climb model, the TEM was used to observe the dynamics of both isolated and interacting SIA loops in ultra-high purity α -Fe (RRR: 7900) and high-purity α -Fe (RRR: 2000, purity: 99.998 wt.%). Thin foils with thickness less than 0.08 mm were pre-annealed at 773 K for 0.5 hours under a vacuum of 3×10^{-6} Pa and at 1073 K for 2 hours under a hydrogen atmosphere at 1 atm to reduce dislocation density and remove any residual stress

before electro-polishing. In the TEM-visible regions, the residual-dislocation density was less than 10^9m^{-2} , allowing the observation of individual loops with negligible effect from the stress field of residual dislocations. Loops were introduced through high-energy electron irradiation, using an ultra-high voltage TEM H-3000 by Hitachi, operated at an acceleration voltage of 2000 kV. The irradiation was performed with a beam dose of $1 \times 10^{25}e/m^2$ at 290K and $1 \times 10^{25}e/m^2$ at 150K, producing SIAs that agglomerated to form loops. Loops were observed using a diffraction-contrast technique at an acceleration voltage of 200 kV to avoid additional knock-on displacement, recording at a frame rate of 30s^{-1} with a Gatan 676 camera.

An isolated $\mathbf{b} = a[100]$ SIA loop of radius $R \simeq 3.8 \pm 0.3\text{nm}$ was observed freely diffusing both along *and* perpendicular to its Burgers vector of $[100]$. We identify the perpendicular motion along $[010]$ as a one dimensional projection of self climb in (100) planes. Through analysis of the mean squared displacement along $[010]$ (Figure 3, inset) self climb diffusivities were extracted at five temperatures, from 793K to 806K, which is approximately $0.1E_m^V/k_B T$ or 2% of the melting temperature, i.e. a very low homologous temperature. Figure 3 shows that equation (3), with parameters for a $\langle 100 \rangle$ SIA loop of radius 3.8nm in iron, is able to capture the measured diffusivities to within 10% apart from the measurement at 797K. As a further validation of our model we implemented the self climb mobility law (1) in dislocation dynamics (DD) simulations that allow glide and self climb along with isotropic elastic interactions from Mura's formula[1]. We simulated the various loop coalescence processes that were seen in our experiments and similar observations from other TEM studies in iron[23] and tungsten[9]. In our simulations the climbing loops were either circular or pill shaped, the loop habit planes were assumed to be perpendicular to the Burgers vector and coalescence was assumed to occur instantaneously on contact on the timescale of climb motion, in agreement with TEM observations. For comparison, we also performed the same simulations using a VMC mobility law (Equation 10 in [3])

$$M_{\text{VMC}} = \frac{2\pi\beta\nu e^{-\beta(E_m^V + E_f^V)}}{b^2 \ln(R/b)}, \quad (4)$$

to give an approximate measure of the expected coalescence times if VMC was the only active climb mechanism. The results of these simulations are given in table I. Despite the fact that we did not account for any background elastic field due to the wider defect network, our calculated coalescence times are directly comparable to those seen in experiment, whilst simulations with the VMC mobility (4) overestimate the observed coalescence times by around six orders of magnitude at the temperatures investigated here, highlighting the much higher rate of

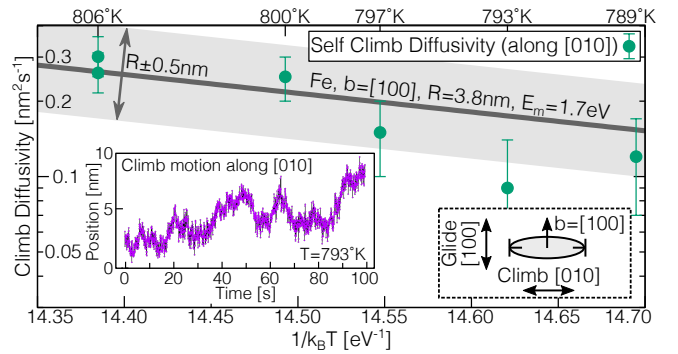
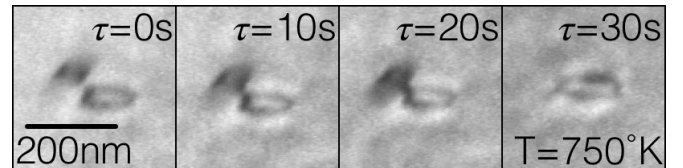


FIG. 3. Self climb diffusivity of an $\langle 100 \rangle$ SIA loop in Fe. The trajectory (observed as a projection on (001) (inset) clearly shows a climb component along $[010]$, perpendicular to the Burgers vector $\mathbf{b} = a[100]$. The predicted self climb diffusivity (3), with vacancy attempt frequency taken from DFT calculations[15] shows good agreement.

self climb and the quality of agreement between equation (3) and experiment. We emphasize that this non-glide motion can only be accounted for by the self climb mechanism developed here. To gauge the importance



	R_1 [nm]	R_2 [nm]	d [nm]	T[K]	τ_{exp} [s]	τ_{scl} [s]	τ_{VMC} [s]
Fe	150	30	70	750	30.0	50.2	3.3×10^7
Fe	3.5	3.5	7	660	~ 0.8	1.8	2.7×10^7
Fe [§]	$\sim 5.$	$\sim 5.$	$\sim 10.$	725	$\sim 6.$	2.1	2.7×10^7
W [†]	20	20	100	1173	66.5	96.2	2.6×10^7
W [†]	100	500*	100	1273	7.	8.6	1.5×10^5

TABLE I. Comparison of coalescence times of $1/2\langle 111 \rangle$ SIA loops from TEM observations (τ_{ex}), DD simulations where loops can glide and self climb (τ_{sc}) and DD simulations where loops can glide and climb via VMC[3] (τ_{VMC}). The self climb model is many orders of magnitude faster than VMC and retains accuracy over a wide range of loop sizes. Above: TEM observation of SIA loops in iron at 750K, corresponding to the first entry in the above table. [§]Data taken from Dudarev et al.[23]. [†]Data taken from Ferroni et al.[9]. * Pill shaped loop, length of $\sim 50\text{nm}$, width $\sim 20\text{nm}$.

of self climb in post-irradiation annealing, we performed glide/self climb DD simulations of SIA loop coarsening, which we compare to an analytical model[7] of VMC loop coarsening that has been shown to be in very good agreement with VMC enabled DD simulations[3]. In our loop coarsening simulations all dislocation loops were taken to be collinear and circular, with coalescence occurring instantaneously on contact, whereupon the larger loop

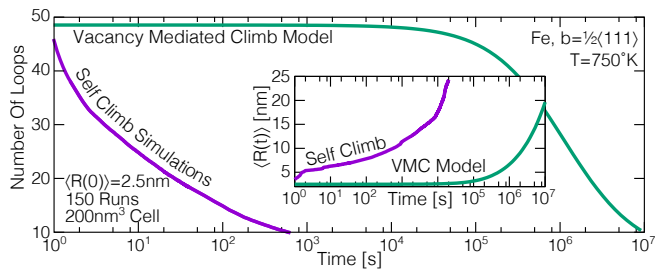


FIG. 4. Self climb enabled dislocation dynamics simulations of SIA loop coarsening, using parameters appropriate for iron at 750K. Our results are compared to an analytical model of VMC loop coarsening, which are in very good agreement with VMC enabled DD simulations[3]. We see that self climb coarsening rates are three to four orders of magnitude greater than those predicted by VMC.

was expanded to accommodate the area of the smaller loop. To accelerate the simulations we used an analytical far field solution for the loop-loop interaction[7] that assumes the distance between loops is greater than the loop radius. Whilst this assumption will clearly break down as loops approach each other, it can be shown that the far field interaction force underestimates the true elastic force, meaning our simulations can be considered to provide a lower bound on the coarsening times. We used simulation parameters appropriate for $1/2\langle 111 \rangle$ SIA loops in iron at 750K in a simulation supercell of $200 \times 200 \times 200$ nm. An initial population of 80 loops were placed randomly in the supercell, with random radii between 1.5nm and 3.5nm, under the constrain that the initial average radius $\langle R(0) \rangle = 2.5$ nm. An ensemble of 150 simulations were performed until less than 4 loops remained in the supercell. In figure 4 we plot the ensemble average time evolution of the loop number $N(t)$ and average loop radius $\langle R(t) \rangle$, along with the predictions of the analytical VMC model, $N(t) = \frac{N(0)}{1+\alpha t}$ and $\langle R(t) \rangle = \langle R(0) \rangle \sqrt{1+\alpha t}$, where $\alpha = \mu a^5 \beta \nu \exp(-\beta[E_m^V + E_f^V]) / \langle R(0) \rangle^2$ [3]. It is clear that the self climb coarsening rates are around three to four orders of magnitude faster than those predicted by VMC, emphasizing the necessity of including the self climb mobility law (1) into simulations of post-irradiation annealing. Our results show that the self climb motion of dislocation loops occurs at a rate comparable to that of impurity segregation or depinning of dislocations[24] and thus is an essential component in models of microstructural evolution, even at low to intermediate homologous temperatures.

We acknowledge grant 633053 from the European Union's Horizon 2020 research and innovation program, grant EP/I501045 from the RCUK Energy Program, grants 15H04244 and 15K14109 from JSPS KAKENHI and 'Advanced Characterization Nanotechnology Platform, Nanotechnology Platform Program' of the Ministry of Education, Culture, Sports, Science and Technology

(MEXT), Japan, at the Research Centre for Ultra-High Voltage Electron Microscopy (Nanotechnology Open Facilities) in Osaka University. The views and opinions expressed herein do not necessarily reflect those of the European Commission.

- [1] J. P. Hirth and J. Lothe, *Theory Of Dislocations* (Malabar, FL Krieger, 1991).
- [2] D. Mordehai, E. Clouet, M. Fivel, and M. Verdier, *Philosophical Magazine* **88**, 899 (2008).
- [3] B. Bakó, E. Clouet, L. M. Dupuy, and M. Blétry, *Philosophical Magazine* **91**, 3173 (2011).
- [4] S. M. Keralavarma, T. Cagin, A. Arsenlis, and A. A. Benzerga, *Physical Review Letters* **109**, 265504 (2012).
- [5] D. Maher and B. Eyre, *Philosophical Magazine* **23**, 409 (1971).
- [6] J. Silcox and M. Whelan, *Philosophical Magazine* **5**, 1 (1960).
- [7] B. Burton and M. Speight, *Philosophical Magazine A* **53**, 385 (1986).
- [8] X. Yi, A. Sand, D. Mason, M. Kirk, S. Roberts, K. Nordlund, and S. Dudarev, *EPL (Europhysics Letters)* **110**, 36001 (2015).
- [9] F. Ferroni, X. Yi, K. Arakawa, S. P. Fitzgerald, P. D. Edmondson, and S. G. Roberts, *Acta Materialia* **90**, 380 (2015).
- [10] F. Kroupa and P. Price, *Philosophical Magazine* **6**, 243 (1961).
- [11] B. Eyre, M. Loretto, and R. Smallman, *Metal Science* **12**, 35 (1978).
- [12] S. Khare and T. Einstein, *Physical Review B* **54**, 11752 (1996).
- [13] D. Nguyen-Manh, A. Horsfield, and S. Dudarev, *Physical Review B* **73**, 020101 (2006).
- [14] H. Sheng, M. Kramer, A. Cadien, T. Fujita, and M. Chen, *Physical Review B* **83**, 134118 (2011).
- [15] N. Sandberg, Z. Chang, L. Messina, P. Olsson, and P. Korzhavyi, *Phys. Rev. B* **92**, 184102 (2015).
- [16] L. Bukonte, T. Ahlgren, and K. Heinola, *Journal of Applied Physics* **115**, 123504 (2014), <http://dx.doi.org/10.1063/1.4869497>.
- [17] S. Plimpton, *Journal Computational Physics* **117**, 1 (1995).
- [18] P. A. Gordon, T. Neeraj, and M. I. Mendeleev, *Philosophical Magazine* **91**, 3931 (2011).
- [19] M. C. Marinica, L. Ventelon, M. R. Gilbert, L. Proville, S. L. Dudarev, J. Marian, G. Bencteux, and F. Willaime, *Journal of Physics: Condensed Matter* **25**, 395502 (2013).
- [20] G. Henkelman, B. P. Uberuaga, and H. Jonsson, *The Journal of Chemical Physics* **113**, 9901 (2000).
- [21] M. Leetmaa and N. V. Skorodumova, *Computer Physics Communications* **185**, 2340 (2014).
- [22] T. D. Swinburne, S. L. Dudarev, S. P. Fitzgerald, M. R. Gilbert, and A. P. Sutton, *Physical Review B* **87**, 64108 (2013).
- [23] S. Dudarev, K. Arakawa, X. Yi, Z. Yao, M. Jenkins, M. Gilbert, and P. Derlet, *Journal of Nuclear Materials* **455**, 16 (2014).
- [24] K. Arakawa, K. Ono, M. Isshiki, K. Mimura, M. Uchikoshi, and H. Mori, *Science* **318**, 956 (2007).